IOPscience iopscience.iop.org

Home Search Collections Journals About Contact us My IOPscience

Improved light management in a-Si:H/a-$Si_{1-x}Ge_x$:H tandem cells by employing multi-functional n-type microcrystalline silicon oxide

This content has been downloaded from IOPscience. Please scroll down to see the full text.

2014 Jpn. J. Appl. Phys. 53 05FV09

(http://iopscience.iop.org/1347-4065/53/5S1/05FV09)

View the table of contents for this issue, or go to the journal homepage for more

Download details:

IP Address: 140.113.38.11
This content was downloaded on 25/12/2014 at 02:51

Please note that terms and conditions apply.

Japanese Journal of Applied Physics 53, 05FV09 (2014) REGULAR PAPER
http://dx.doi.org/10.7567/JJAP.53.05FV09

Improved light management in a-Si:H/a-$Si_{1-x}Ge_x$:H tandem cells by employing multi-functional n-type microcrystalline silicon oxide

Hung-Jung Hsu*, Shin-Wei Liang, Yen-Tang Huang, Cheng-Hang Hsu, and Chuang-Chuang Tsai

Department of Photonics, National Chiao Tung University, Hsinchu, Taiwan 300, R.O.C.
E-mail: bear0300022@gmail.com

Received November 30, 2013; accepted February 28, 2014; published online April 22, 2014

In this work, the development of plasma-enhanced chemical vapor deposition (PECVD) μc-SiO_x:H(n) and its application to a-Si:H/a-$Si_{1-x}Ge_x$:H tandem cells as the intermediate reflecting layer (IRL) and back reflector (BR) is presented. The n-type microcrystalline silicon oxide [μc-SiO_x:H(n)] was used as multifunctional layers in silicon thin-film solar cells owing to its wide bandgap and low refractive index. In the development of μc-SiO_x:H(n), increasing RF power increased film oxygen content, which widened the bandgap while reducing dark conductivity. Applying the μc-SiO_x:H to a-Si:H/a-$Si_{1-x}Ge_x$:H tandem cells as IRL and BR significantly improved cell performance. The μc-SiO_x:H(n) IRL increases the current of the top cell, thus improving the light management in a-Si:H/a-$Si_{1-x}Ge_x$:H tandem cells. On the other hand, the μc-SiO_x:H(n) can be used as the BR replacing the n-type a-Si:H and ITO layers. The μc-SiO_x:H increased cell conversion efficiency by 12.9% as IRL, and by 9.7% as BR, achieving 10.03% efficiency. © 2014 The Japan Society of Applied Physics

1. Introduction

Hydrogenated amorphous silicon (a-Si:H)-based thin-film solar cells have the potential to be a cost-effective photovoltaic technology owing to its minimal material usage. To stay competitive against other photovoltaic, the conversion efficiency of silicon thin-film solar cells need to be further improved. Typically, the multijunction structure is adopted to improve the utilization of the solar spectrum while increasing the stabilized efficiency of solar cells owing to the decreased absorber thickness.[1] a-Si:H/a-$Si_{1-x}Ge_x$:H tandem cells were reported to have high stabilized conversion efficiency in small scale and module level.[2–5] To further improve the performance of the a-Si:H/a-$Si_{1-x}Ge_x$:H tandem cells, an efficient light management in the cells is necessary.

Conventionally, the light management can be improved by adopting an intermediate reflecting layer (IRL) between the top cell and the bottom cell or by employing an appropriate back reflector (BR).[6–8] As previously reported, IRL functions to increase the current of the top cell without increasing the thickness of the absorber.[7–9] This improves the current balance between the component cells and thus increases cell efficiency. On the other hand, the standard BR comprising a transparent conductive oxide (TCO) layer together with a Ag back contact exhibits an increased reflectance.[6] The increase is likely due to the reduction in absorption loss at the dielectric/Ag interface owing to the low-refractive-index TCO layer which shifted the excitation of surface plasmon resonance to the higher-energy region.[10,11] However, the employment of IRL and TCO/Ag BR requires an additional ex situ sputtering step for the low-refractive-index TCO layer.

In recent years, n-type microcrystalline silicon oxide [μc-SiO_x:H(n)] has been reported as a promising material that can fulfill multiple functions, for example, as the IRL, BR and n-layer of the component cells in a-Si:H and a-Si:H/μc-Si:H solar cells.[12–17] The μc-SiO_x:H was found to be a biphase material containing the conductive μc-Si:H region embedded in the wide-bandgap a-SiO_x:H tissue.[18] The refractive index can be reduced owing to the incorporation of oxygen into the films, generating an amorphous silicon oxide. The conductive crystalline region provides sufficient conductivity along the film growth direction, while the wide-bandgap amorphous tissue offers optical transparency, which reduces the parasitic absorption loss.[17,18] The μc-SiO_x:H(n) was reported to serve as the IRL in a-Si:H/μc-Si:H tandem cells,[12,13] as BR in single-junction or tandem cells,[14,16] as the shunt quenching layer on highly textured substrates,[19] and as the window layer in n-side illuminated n–i–p μc-Si:H solar cells.[20]

In this work, the development of n-type μc-SiO_x:H and its application to a-Si:H/a-$Si_{1-x}Ge_x$:H tandem cells as both IRL and BR were investigated. The optical and electrical properties of μc-SiO_x:H(n) at different RF powers are presented and discussed. The effect of μc-SiO_x:H(n) as IRL and BR on cell performance is discussed in detail.

2. Materials and methods

Silicon-based thin films were prepared in a 27.12 MHz single-chamber plasma-enhanced chemical vapor deposition (PECVD) system with a load-lock transfer chamber. SiH_4, GeH_4, CO_2, B_2H_6, PH_3, and H_2 were used as source gases. The n-type μc-SiO_x:H layer was prepared at an RF power in the range from 30 to 150 W and a CO_2-to-SiH_4 flow ratio of 0.4. The a-Si:H/a-$Si_{1-x}Ge_x$:H tandem solar cells were deposited on the SnO_2:F-coated glass substrates in a p–i–n superstrate configuration. A bandgap-graded absorber was employed in the a-$Si_{1-x}Ge_x$:H bottom cell. The preparation and details of bandgap-graded absorber was reported in our previous work.[21] The photo conductivity of the bandgap-graded layers decreased from 1.2×10^{-5} to 3.1×10^{-6} S/cm, while the dark conductivity remained at approximately 4×10^{-10} S/cm with decreasing bandgap of a-$Si_{1-x}Ge_x$:H from 1.75 to 1.53 eV.

The structural variation of μc-SiO_x:H was characterized by Raman spectroscopy using a probe laser at a wavelength of 488 nm. Film oxygen content was characterized by X-ray photoelectron spectroscopy (XPS) with precleaning for each sample. The optical bandgap E_{04} (the photon energy at which the absorption coefficient is 10^4 cm^{-1}) was obtained by UV–vis spectroscopy. Coplanar conductivity was measured at an electrode spacing of 0.8 mm. External quantum efficiency (EQE) was characterized under short-circuit condition. The current density–voltage (J–V) characteristics of a-$Si_{1-x}Ge_x$:H single-junction solar cells were obtained by

 © 2014 The Japan Society of Applied Physics

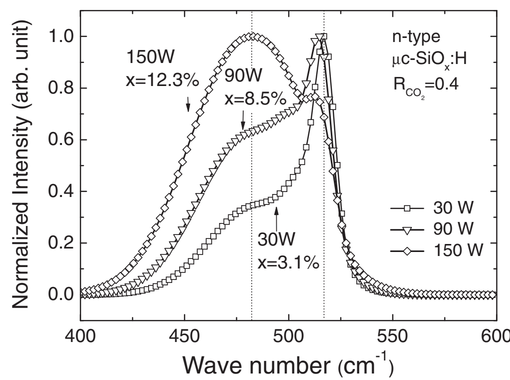

Fig. 1. Raman spectra of n-type μc-SiO$_x$:H films prepared at different RF powers. The film oxygen content (x) is also shown.

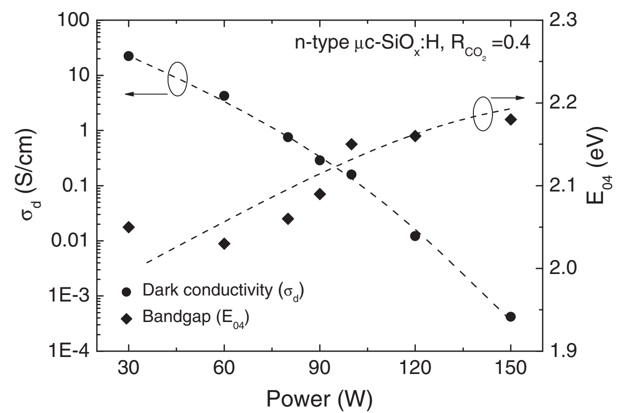

Fig. 2. Dark conductivities and optical bandgaps (E_{04}) of n-type μc-SiO$_x$:H films prepared at different RF powers.

J–V measurement under illumination by an AM1.5G light source with an electrode area of 0.25 cm^2.

3. Results and discussion

3.1 Effect of RF power on the optoelectrical properties of n-type μc-SiO$_x$:H films

To study the structural variation of n-type μc-SiO$_x$:H [μc-SiO$_x$:H(n)] prepared at different RF powers, Raman analysis was conducted. The normalized Raman spectra of μc-SiO$_x$:H(n) prepared at different RF powers are shown in Fig. 1. As can be seen, the film prepared at 30 W exhibited a predominant c-Si peak at 520 cm^{-1}, a tail containing a broad a-Si:H peak centered at 480 cm^{-1}, and a defective c-Si peak centered at 510 cm^{-1}.[22] As the power increased from 30 to 150 W, a relative increase in the a-Si:H peak compared with the c-Si peak was observed, indicating that the crystalline volume fraction decreased. On the other hand, the film oxygen content (x) increased from 3.1 to 12.3% as the power increased. This may be due to the higher-energy plasma that enhanced the dissociation of CO_2 in the gas phase, which in turn enhanced oxygen incorporation.[23] Since μc-SiO$_x$:H was reported to be a biphase material consisting of the conductive μc-Si:H region embedded in the a-SiO$_x$:H tissue, the incorporation of oxygen into the film enhanced the a-SiO$_x$:H phase and also the structural disorder, which decreased the crystalline volume fraction.[17,18] As a consequence, the increase in power increased film oxygen content while reducing the crystalline volume fraction of μc-SiO$_x$:H(n).

To determine the correlation between the structural variation and the electrical properties of μc-SiO$_x$:H(n) prepared at different powers, dark conductivity was measured. The dependence of the dark conductivity σ_d and optical bandgap E_{04} of μc-SiO$_x$:H(n) films on different powers is shown in Fig. 2. As the power increased from 30 to 150 W, the dark conductivity decreased substantially from 2.23×10^1 to 4.21×10^{-4} S/cm, accompanied by the increase in E_{04} from 2.05 to 2.18 eV. The increase in E_{04} was due to the enhanced a-SiO$_x$:H phase arising from the increased film oxygen content (Fig. 1). On the other hand, the decrease in dark conductivity was due to the reduced crystalline volume fraction, the widened bandgap, and the enhanced a-SiO$_x$:H phase having a low doping efficiency as the film oxygen content increased (Fig. 1). As a result, increasing the power enhanced the incorporation of oxygen into the film, which widened the bandgap while reducing the crystalline volume fraction and thus decreasing the dark conductivity.

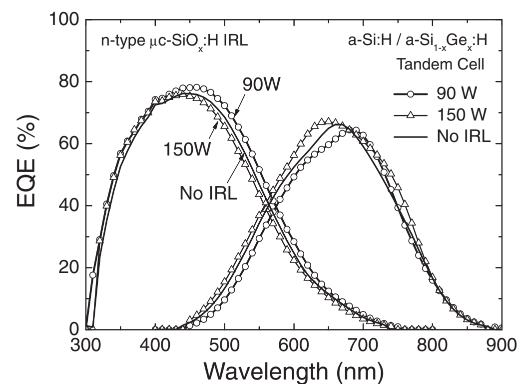

Fig. 3. EQE of a-Si:H/a-Si$_{1-x}$Ge$_x$:H tandem cells fabricated employing n-type μc-SiO$_x$:H IRL prepared at different RF powers. The EQE of a tandem cell without IRL is shown for comparison.

3.2 Effect of μc-SiO$_x$:H intermediate reflecting layer prepared at different RF powers on the performance of a-Si:H/a-Si$_{1-x}$Ge$_x$:H tandem cells

In this section, the influence of μc-SiO$_x$:H IRL on the performance of a-Si:H/a-Si$_{1-x}$Ge$_x$:H tandem cells was investigated. Figure 3 shows the EQE of the tandem cells with μc-SiO$_x$:H IRL prepared at different RF powers. The tandem cell without IRL (solid line) is also shown for comparison. In the case of using the μc-SiO$_x$:H IRL prepared at 90 W, the EQE of the top cell increased while the EQE of the bottom cell decreased accordingly compared with that of the cell without IRL. This can be due to the μc-SiO$_x$:H having a lower refractive index than adjacent layers, reflecting photons back to the top cell.[12,13] The internal reflection due to the refractive index difference transferred the current from the bottom cell to the top cell and thus improved the current matching between the component cells. In contrast, in the case of using the μc-SiO$_x$:H IRL prepared at 150 W, the EQE of the top cell decreased while the EQE of the bottom cell increased, as compared with that of the cell with μc-SiO$_x$:H IRL prepared at 90 W. The larger refractive index contrast arising from the higher oxygen content ($x =$ 12.3%) of μc-SiO$_x$:H prepared at 150 W (Fig. 2) seemed to

© 2014 The Japan Society of Applied Physics

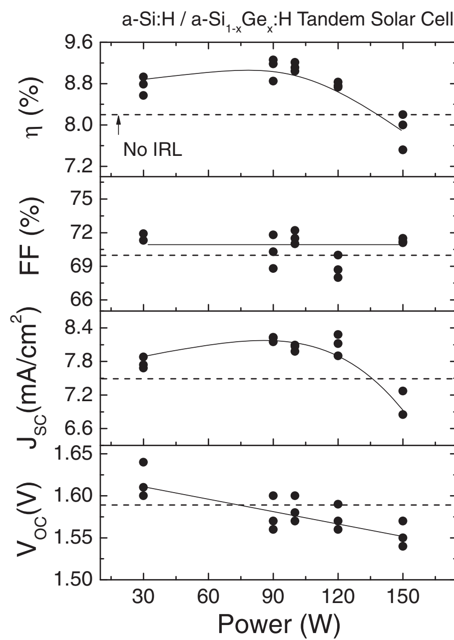

Fig. 4. Performance of a-Si:H/a-$Si_{1-x}Ge_x$:H tandem cells fabricated employing n-type μc-SiO_x:H IRL prepared at different RF powers. The dotted line denotes the performance of the tandem cell without IRL.

result in no significant increase in the EQE of top cell. The reduced EQE in the top cell can thus be attributed to the low conductivity (4.21×10^{-4} S/cm) of μc-SiO_x:H prepared at 150 W (Fig. 2), which obstructed the electron transport from the top cell. This led to the lower EQE in the top cell. On the other hand, the higher EQE in the bottom cell can be ascribed to the larger bandgap (2.18 eV) of μc-SiO_x:H IRL, which reduced the parasitic absorption loss in the doped layer. As a result, the a-Si:H/a-$Si_{1-x}Ge_x$:H tandem cell with μc-SiO_x:H IRL prepared at 90 W ($x = 8.5\%$) exhibited sufficient internal reflection and improved the light management.

The performance of a-Si:H/a-$Si_{1-x}Ge_x$:H tandem cells with μc-SiO_x:H IRL prepared at different RF powers is shown in Fig. 4. The dotted line represented the performance of the tandem cell without μc-SiO_x:H IRL. As can be seen from the figure, the V_{OC} exhibited a monotonic reduction from 1.62 to 1.53 V (average value) as the power increased from 30 to 150 W. This can be due to the degraded carrier recombination at the n/p junction resulting from worsened carrier transport owing to the reduction in the conductivity of μc-SiO_x:H IRL. On the other hand, an increased J_{SC} in the range from 7.8 to 8.1 mA/cm^2 was observed for the cells with μc-SiO_x:H IRL prepared at powers in the range from 30 to 120 W, as compared with the cell without IRL where the J_{SC} was limited by the top cell with a J_{SC} of 7.4 mA/cm^2. The increased J_{SC} due to the increased EQE in the top cell came from the internal reflection by the μc-SiO_x:H IRL with a decreased refractive index (Fig. 3). The tandem cell with μc-SiO_x:H IRL prepared at a power in the range from 30 to 120 W exhibited an increase in efficiency by 0.7% compared with the cell without IRL owing to the improved current matching without an increase in the thickness of the top cell.

Moreover, the J_{SC} exhibited an increase from 7.77 to 8.20 mA/cm^2 as the power increased from 30 to 90 W. This was due to the increase in EQE of the top cell (the current-

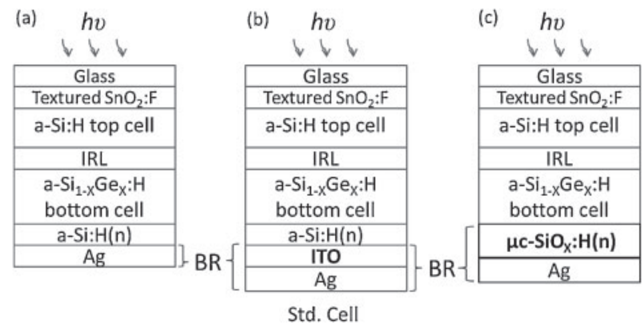

Fig. 5. Cross-sectional structures of a-Si:H/a-$Si_{1-x}Ge_x$:H tandem cells with (a) Ag, (b) ITO/Ag (standard cell), and (c) μc-SiO_x;H(n)/Ag as BR.

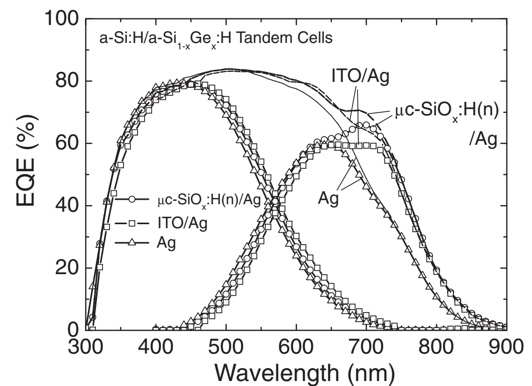

Fig. 6. EQE of a-Si:H/a-$Si_{1-x}Ge_x$:H tandem cells fabricated employing different BR.

limiting cell) owing to the use of the μc-SiO_x:H IRL with a high oxygen content as well as low refractive index.[16,24] However, a further increase in the power to 150 W reduced the J_{SC} to 7.13 mA/cm^2. The reduction was due to the decreased EQE in the top cell, as demonstrated in Fig. 3. Consequently, by carefully tuning the optical and electrical properties of the μc-SiO_x:H layer, the μc-SiO_x:H can function well as the IRL. A higher efficiency of 9.26% was obtained in the cell with μc-SiO_x:H IRL prepared at 90 W than in the cell without IRL (8.20%), which is a relative increase of 12.9%.

3.3 Tandem cells employing dual-function n-type μc-SiO_x:H as BR

In this section, the effect of μc-SiO_x:H(n) as the BR on the performance of the a-Si:H/a-$Si_{1-x}Ge_x$:H tandem cells was investigated. Figure 5 demonstrates the cross-sectional structures of a-Si:H/a-$Si_{1-x}Ge_x$:H tandem cells with different BR. The term BR was defined as dielectric/Ag bilayers in this work. The refractive index (at a wavelength of 650 nm) and E_{04} of μc-SiO_x:H(n) were 3.2 and 2.2 eV, respectively. The μc-SiO_x:H(n) served as the replacement for the n-type a-Si:H layer and the subsequent ITO layer in our standard tandem cell.

The EQE of the tandem cells with different BRs are illustrated in Fig. 6. As the ITO layer was inserted at the interface of a-Si:H(n)/Ag, the EQE at wavelengths from 650 to 900 nm significantly increased with respect to the cell with a-Si:H(n)/Ag as BR. The increase was possibly due to the shift of the plasmonic resonance peak to the higher-energy region owing to the lower refractive index of ITO layer,

© 2014 The Japan Society of Applied Physics

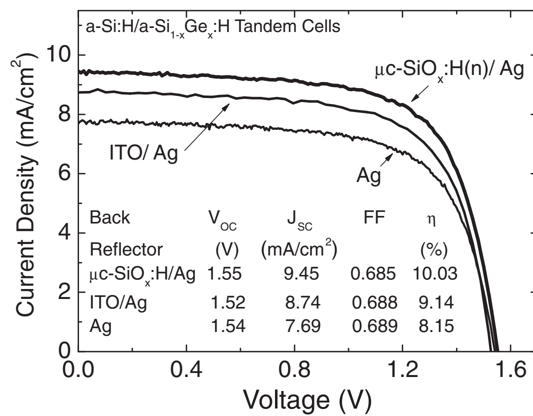

Fig. 7. *J–V* characteristics and performance of a-Si:H/a-$Si_{1-x}Ge_x$:H tandem cells with different BRs.

which reduced the optical absorption loss at the a-Si:H(n)/Ag interface.[11] On the other hand, as the μc-SiO_x:H(n)/Ag was employed, the EQE at wavelengths from 600 to 900 nm substantially increased compared with the EQE of the cell with a-Si:H(n)/Ag as BR. This suggests that the μc-SiO_x:H(n)/Ag can function well as BR with a similar effect to the ITO/Ag. Moreover, in comparison with the cell with a-Si:H(n)/ITO as BR, the cell with μc-SiO_x:H(n)/Ag exhibited a higher EQE at wavelengths from 600 to 750 nm. This can be ascribed to the reduced parasitic absorption loss in the n-type μc-SiO_x:H layer with a larger bandgap than in the a-Si:H n-layer.

The *J–V* characteristics and performance of tandem cells with different BRs are illustrated in Fig. 7. Each top cell thickness was carefully tuned to match the current generated from bottom cell with different BRs. As can be seen, the FF and V_{OC} seemed not to be markedly influenced by the different BRs. As the standard ITO/Ag BR was employed, the J_{SC} was substantially increased from 7.69 to 8.74 mA/cm^2 compared with the cell with a-Si:H(n)/Ag. The increase was due to the increased current density of the bottom cell (Fig. 6) which increased the total current density of the tandem cell. On the other hand, as the μc-SiO_x:H(n)/Ag was employed, the J_{SC} was substantially increased from 7.69 to 9.45 mA/cm^2 than the cell with a-Si:H(n)/Ag. This was also due to the increased current density in the bottom cell with a similar effect to ITO/Ag BR, as shown in Fig. 6. In comparison with the standard ITO/Ag BR, the cell with the particular μc-SiO_x:H(n)/Ag structure exhibited a further increase in J_{SC} by 0.71 mA/cm^2, which corresponded to a relative increase in 8.1%. The μc-SiO_x:H(n) exhibited dual functions as both the BR of the tandem cell and the n-layer of the bottom cell. The μc-SiO_x:H(n) used as the BR increased cell conversion efficiency by 9.7% compared with the standard ITO/Ag BR. This multifunctional n-type μc-SiO_x:H can simplify fabrication process and reduce contamination at the n-layer/Ag interface owing to the non-necessity of the back TCO sputtering process. As a consequence, the a-Si:H/a-$Si_{1-x}Ge_x$:H tandem cell fabricated employing μc-SiO_x:H(n)/Ag BR obtained an efficiency of 10.03% with V_{OC} of 1.55 V, J_{SC} of 9.45 mA/cm^2, and FF of 68.5%. Further improvement of the cell performance is expected with the use of the μc-SiO_x:H with a higher oxygen content.

4. Conclusions

In this paper, we presented the development of n-type μc-SiO_x:H and its application to a-Si:H/a-$Si_{1-x}Ge_x$:H tandem cells as the intermediate reflecting layer (IRL) and back reflector (BR). In the development of μc-SiO_x:H films, the increase in RF power increased the film oxygen content, which widened the bandgap owing to the power-assisted CO_2 dissociation. This in turn reduced the crystalline volume fraction and the dark conductivity of μc-SiO_x:H(n). Applying n-type μc-SiO_x:H to a-Si:H/a-$Si_{1-x}Ge_x$:H tandem cells as IRL and BR significantly improved the cell performance. The use of IRL for μc-SiO_x:H(n) prepared at 90 W increased the current density of the top cell, thus improving the light management in a-Si:H/a-$Si_{1-x}Ge_x$:H tandem cells. On the other hand, the μc-SiO_x:H(n) can also be used as BR to replace the n-type a-Si:H and ITO layers. This allows for an all-in situ process resulting in process simplification. The μc-SiO_x:H increased cell conversion efficiency by 12.9% as IRL and by 9.7% as the BR, achieving 10.03% efficiency.

Acknowledgement

This work was financially sponsored by the National Science Council under grant number 102-3113-P-008-001.

1) S. Guha, MRS Proc. **149**, 405 (1989).
2) J. Yang and S. Guha, Appl. Phys. Lett. **61**, 2917 (1992).
3) S. Guha, X. Xu, J. Yang, and A. Banerjee, Appl. Phys. Lett. **66**, 595 (1995).
4) S. Okamoto, E. Maruyama, A. Terakawa, W. Shinohara, S. Nakano, Y. Hishikawa, K. Wakisaka, and S. Kiyama, Sol. Energy Mater. Sol. Cells **66**, 85 (2001).
5) E. Maruyama, S. Okamoto, A. Terakawa, W. Shinohara, M. Tanaka, and S. Kiyama, Sol. Energy Mater. Sol. Cells **74**, 339 (2002).
6) J. Springer, B. Rech, W. Reetz, J. Müller, and M. Vanecek, Sol. Energy Mater. Sol. Cells **85**, 1 (2005).
7) P. Obermeyer, C. Haase, and H. Stiebig, Appl. Phys. Lett. **92**, 181102 (2008).
8) C. Rockstuhl, F. Lederer, K. Bittkau, T. Beckers, and R. Carius, Appl. Phys. Lett. **94**, 211101 (2009).
9) J. Krc and F. Smole, Sol. Energy Mater. Sol. Cells **86**, 537 (2005).
10) J. Springer, A. Poruba, L. Mullerova, M. Vanecek, O. Kluth, and B. Rech, J. Appl. Phys. **95**, 1427 (2004).
11) F. J. Haug, T. Soderstrom, O. Cubero, V. Terrazzoni-Daudrix, and C. Ballif, J. Appl. Phys. **104**, 064509 (2008).
12) P. Buehlmann, J. Bailat, D. Dominé, A. Billet, F. Meillaud, A. Feltrin, and C. Ballif, Appl. Phys. Lett. **91**, 143505 (2007).
13) C. Das, A. Lambertz, J. Huepkes, W. Reetz, and F. Finger, Appl. Phys. Lett. **92**, 053509 (2008).
14) P. D. Veneri, L. V. Mercaldo, and I. Usatii, Appl. Phys. Lett. **97**, 023512 (2010).
15) P. D. Veneri, L. V. Mercaldo, and I. Usatii, Prog. Photovoltaics **21**, 148 (2013).
16) B. Janthong, A. Hongsingthong, T. Krajangsang, L. Zhang, P. Sichanugrist, and M. Konagai, J. Non-Cryst. Solids **358**, 2478 (2012).
17) A. Lambertz, T. Grundler, and F. Finger, J. Appl. Phys. **109**, 113109 (2011).
18) P. Cuony, M. Marending, D. Alexander, M. Boccard, G. Bugnon, M. Despeisse, and C. Ballif, Appl. Phys. Lett. **97**, 213502 (2010).
19) M. Despeisse, G. Bugnon, A. Feltrin, M. Stueckelberger, P. Cuony, F. Meillaud, A. Billet, and C. Ballif, Appl. Phys. Lett. **96**, 073507 (2010).
20) V. Smirnov, W. Böttler, A. Lambertz, H. Wang, R. Carius, and F. Finger, Phys. Status Solidi C **7**, 1053 (2010).
21) H.-J. Hsu, C.-H. Hsu, and C.-C. Tsai, Int. J. Photoenergy **2013**, 364638 (2013).
22) C. Droz, E. Vallat-Sauvain, J. Bailat, L. Feitknecht, J. Meier, and A. Shah, Sol. Energy Mater. Sol. Cells **81**, 61 (2004).
23) S. Iftiquar, J. Phys. D **31**, 1630 (1998).
24) A. Lambertz, V. Smirnov, T. Merdzhanova, K. Ding, S. Haas, G. Jost, R. E. I. Schropp, F. Finger, and U. Rau, Sol. Energy Mater. Sol. Cells **119**, 134 (2013).

© 2014 The Japan Society of Applied Physics